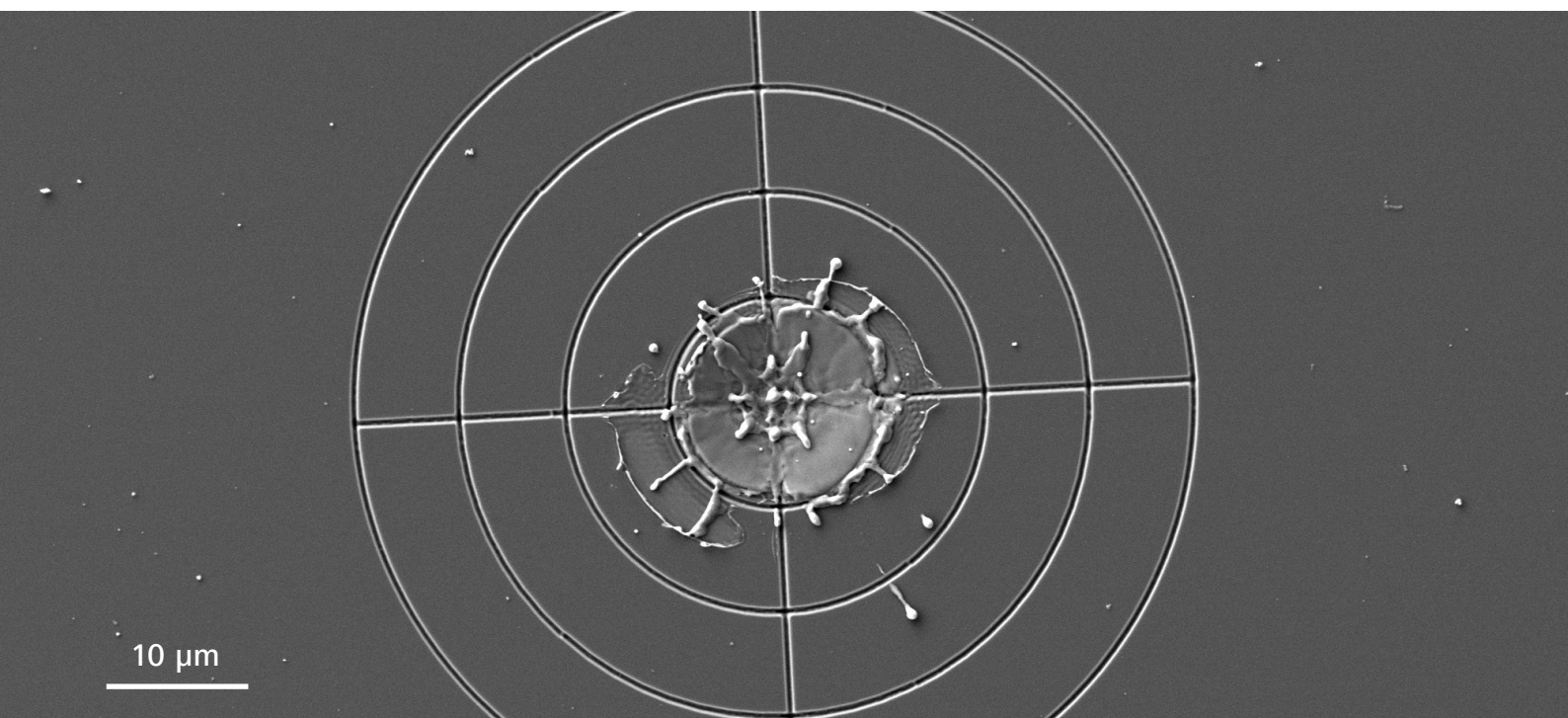


Targeted Sample Preparation with ZEISS Crossbeam laser



Seeing beyond

In this technical note, we describe how site-specific laser work is done with ZEISS Crossbeam laser. After locating the region of interest (ROI) under SEM observation, the coordinates of the ROI are transferred to the laser system following a correlative approach. This allows targeting of the ROI with a precision better than 15 μm . This value can be further reduced locally to less than 2 μm by applying an improved registration protocol enabling more efficient workflows.

Introduction

Laser micromachining is a well-established technique in industry. Lasers are used to mark, drill, and cut workpieces with very high precision [1]. With the availability of ultrashort pulsed lasers, laser-based solutions are finding increasing adoption in the field of sample preparation for microscopy. For this purpose, stand-alone lasers [2] as well as integrations with FIB-SEM instruments, so-called LaserFIBs, have recently been commercialized [3,4].

Ultrashort laser pulses in the femtosecond (fs) range produce minimal sample damage and heat-affected zones (HAZ). At the same time, fs lasers allow very fast and precise material removal. As an example, the fs laser used on ZEISS Crossbeam laser can remove up to 15 mio μm^3 of silicon per second with a probe size of $<15 \mu\text{m}$ diameter.

Figure 1 shows ZEISS Crossbeam laser. The laser work is done in a separate dedicated chamber (in the foreground) to avoid contamination of the FIB-SEM main chamber. During work, the sample is shuttled between the laser and the main chambers. Site-specific work is done by simply handshaking SEM and laser coordinates.

In this technical note, we describe the coordinate registration process and how it can be improved to ensure laser targeting of the ROI with $<2 \mu\text{m}$ precision for local areas. Such precision allows milling closer to the ROI by laser, reducing subsequent FIB processing time and thus overall time-to-result.

Laser Registration

The Crossbeam laser workflow for a site-specific preparation is shown schematically in Figure 2. The sample is mounted on a special sample holder (see inset) with four distinct fiducials which are used for registration purposes as described in the following.



Figure 1: ZEISS Crossbeam laser.

The first step is to locate the ROI (or multiple ROIs) in the SEM (Fig. 2A). This is a non-trivial step because the ROI is usually buried deeply under the surface. We assume that the coordinates of the ROI are known based either on the structure of the sample itself (e.g. an interface in a layered system), a CAD layout, or a previous characterization by a non-destructive 3D imaging technique e.g. CT or X-ray microscopy (XRM). The 3D CAD or XRM data is imported into the FIB-SEM user interface and correlated with the SEM image of the surface. The target coordinates translate into a certain SEM stage position, location on the SEM image, and depth. As a reference, the SEM image is acquired at the location of the ROI using a suitable magnification, as required later for precise positioning of the laser milling pattern.

Next, alignment of the sample holder and SEM coordinate systems is accomplished by automatically centering the four sample holder fiducials under SEM observation (Fig. 2B). By doing this, the relative position of the ROI with respect to the fiducials is determined.

For laser work, the sample is now transferred to the laser preparation chamber attached to the airlock (Fig. 2C). In a second registration step (Fig. 2D), the laser scans small areas around the four fiducials to measure their exact position in the coordinate system of the laser scanning unit. This locks the laser and SEM coordinate systems. Thus, laser patterning objects can be placed on the previously recorded SEM image of the ROI and exposed (Fig. 2E).

In order to continue FIB-SEM work after laser milling, the sample is returned to the main chamber of the instrument completing the workflow (Fig. 2F).

The workflow just described allows targeting a feature within an area of 25 mm × 25 mm [5] with an accuracy of <15 μm. This value is equal to the laser beam diameter and can be further improved by performing local offset corrections as will be described in the following section.

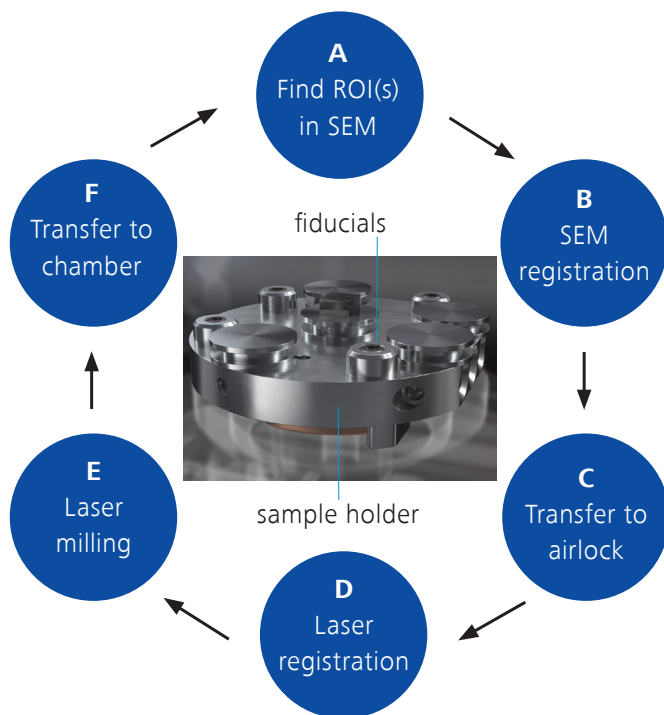


Figure 2: The Crossbeam laser workflow for site-specific preparation shown schematically.

Improving Laser Accuracy With Local Offset Corrections

Let us consider the main sources of error that limit the targeting accuracy of the laser. These are connected to errors in:

1. SEM registration
2. Laser registration
3. Laser scan field calibration

For a given SEM registration, the first error remains constant as long as the position of the sample with respect to the fiducials of the sample holder (inset of Fig. 2) is not changed. The third error is dependent on the uniformity of the laser projection optics and on the laser focus, i.e. on the height of the sample. Using a local offset correction specific to the sample and area of work, errors 1 and 3 can be determined experimentally and corrected for. Thus, the only remaining source of error is the laser registration. Within an area of approximately 1 mm × 1 mm around the ROI, the residual error is <2 μm, as will be shown in the next section.

Figure 3 illustrates how the local offset correction method works.

For this example, the sample is a piece of silicon wafer. A fictitious ROI was protected with an ion-beam-induced deposition (IBID) of carbon (Fig. 3a). The IBID is square with a nominal side length of 2 μm. Next to the ROI, two fiducials were machined by FIB. Alternatively, any distinct features on the sample could have been used.

The complete process illustrated in Figure 2 was conducted once aiming for the left fiducial. As shown in Figure 3b, the target was missed by $|\Delta x| = 2.17 \mu\text{m}$ in the x- and $|\Delta y| = 0.53 \mu\text{m}$ in the y-direction (measured as the distance between the centers of the target and the circular outline of the laser spot). The laser scan field calibration was then corrected by simply adding Δx and Δy as an offset. To further refine this offset correction, a second iteration was done. This time the right fiducial was targeted, skipping step B of the workflow (see Fig. 2), i.e. preserving the SEM registration. Figure 3c shows the result. The targeting accuracy was further improved. A new offset of $(|\Delta x|, |\Delta y|) = (0.34 \mu\text{m}, 1.62 \mu\text{m})$ was measured and corrected for. As discussed in the next section, additional iterations are not needed as they would not improve the targeting accuracy any further. After the two local offset corrections, laser machining around the ROI can be performed with a precision better than $\pm 2 \mu\text{m}$.

The time added by the local offset corrections is around 10 min for the single and less than 15 min for the double local offset correction.

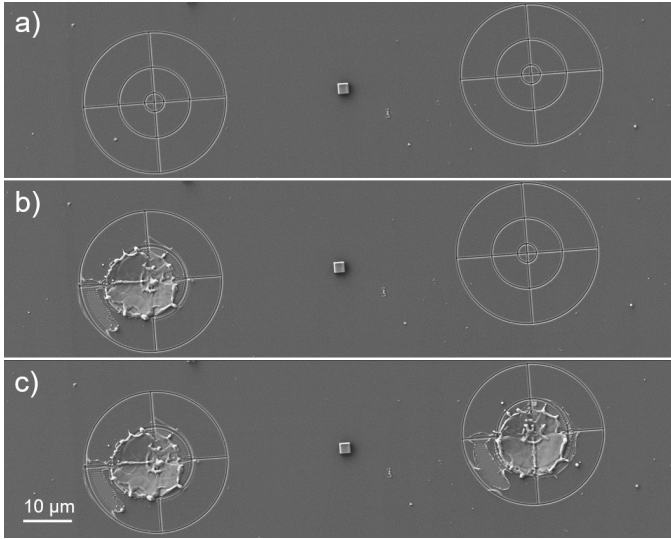


Figure 3: Illustration of the local offset correction method: a) Two FIB-machined targets were patterned near the ROI. The SEM image a) was used as a reference to guide the laser. b) The offset between SEM and laser is measured and corrected for (first offset correction). c) The second fiducial was targeted to further refine the local offset correction (second offset correction).

Quantifying the Laser Targeting Accuracy

To quantify and get more statistics about the achievable laser targeting accuracy, the following experiment was performed.

An array of 3 × 3 fiducials was machined on a silicon chip by FIB to provide nine test sites. The fiducials consist of a cross and two concentric circles as shown in the inset of Figure 4. The inner circle has a radius of 2 µm, which corresponds to the targeting accuracy specification using a double local offset correction. The outer circle has a diameter of 15 µm, i.e. the nominal spot size of the fs laser beam. An SEM image of each fiducial was acquired and stored as an ROI for the laser experiment.

A first frame 80 µm × 80 µm in size was machined by laser around a fiducial outside the array following the workflow in Figure 2. The targeting accuracy was determined as shown exemplarily in Figure 4 by simply measuring the distance $d = \sqrt{(\Delta x)^2 + (\Delta y)^2}$ between the crossing point of the frame diagonals and the center of the FIB fiducial. The local offset correction (Δx , Δy) was applied to the laser scan field calibration. A second local offset correction was done using the top left fiducial of the array (fiducial 1, Table 1) and kept constant for the rest of the experiment.

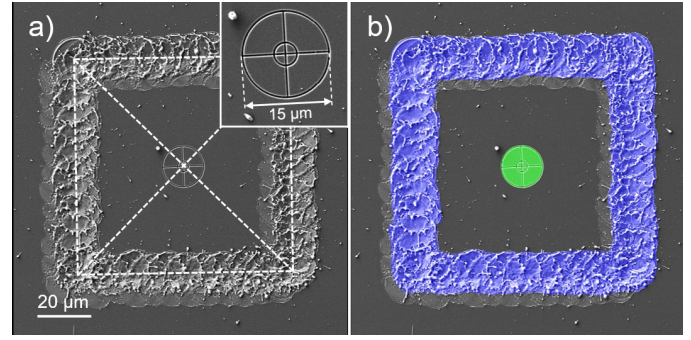


Figure 4: Laser targeting accuracy measurement for one of the fiducials. a) Manual measurement. b) Measurement using automatic segmentation.

Subsequent exposure of laser frames to target all remaining FIB fiducials was done performing a new laser registration before each next exposure. This means for fiducials 2 to 9, the following procedure was iterated:

- Shuttle sample holder to laser preparation chamber.
- Trigger automatic laser registration.
- Center laser frame around the targeted fiducial on the corresponding SEM reference image.
- Expose laser pattern.
- Return sample holder to main chamber to document the result.
- Repeat for next fiducial.

Images documenting the laser milling result after the second, fourth, sixth, and eighth iteration are shown in Figure 5.

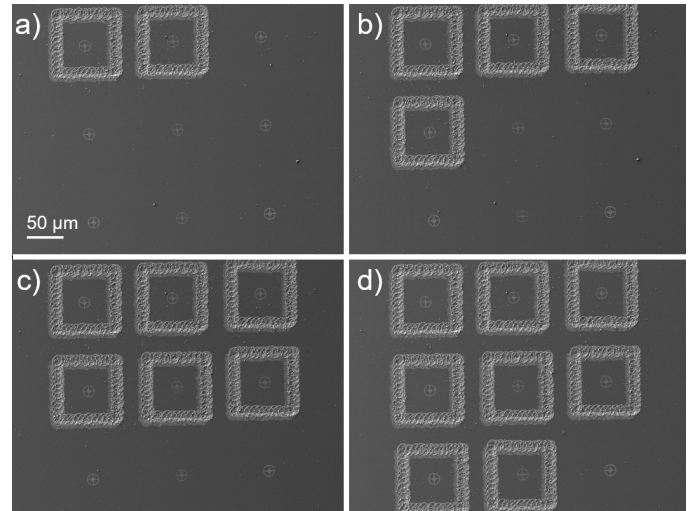


Figure 5: SEM images of a 3 × 3 array of FIB fiducials after laser exposure of a frame around the fiducial number a) 2, b) 4, c) 6, and d) 8.

For an automated user-independent quantification, machine-learning-based segmentation using ZEISS ZEN Intellesis [6] was used to determine the deviation (Δx , Δy) for each fiducial. Three similar images (not part of this experiment to avoid training bias) were used to train a deep-neural network for segmentation of the laser tracks and FIB fiducials. The training was done using the open online image-analysis and machine-learning platform APEER [7]. The network was imported in ZEISS ZEN Intellesis for automated analysis of the SEM images. The output of the segmentation was two objects for the laser track and the FIB fiducial for each image. The coordinates of the centers of mass for both objects were determined. From their difference (Δx , Δy) the distance d was calculated.

Fiducial	Δx	Δy	d
1	3.04	-3.77	4.84
2	0.72	-0.96	1.20
3	1.95	-1.00	2.19
4	-0.68	-1.82	1.94
5	0.11	0.43	0.44
6	-0.93	-0.83	1.25
7	-0.98	-0.25	1.02
8	-1.45	1.20	1.88
9	0.68	-0.62	0.92
Average (2–9)			1.4 ± 0.6

Table 1: Results of the ZEISS ZEN Intellesis analysis for the nine fiducials shown in Figure 5.

The results are summarized in Table 1. Fiducial 1 was used for the local offset correction. The average targeting accuracy was $\bar{d} = (1.4 \pm 0.6) \mu\text{m}$ for fiducials 2–9.

A second experiment was designed to verify that $\bar{d} \leq 2 \mu\text{m}$ is achievable at any location within the laser writing field. A total of four Crossbeam laser systems were surveyed. For each system, nine locations distributed across the central scan field area of $25 \times 25 \text{ mm}$ were considered; see Figure 6. Each site contained an array of fiducials that were targeted by laser as in the previous experiment.

As an example, Figure 7 shows the measured values (Δx , Δy) obtained on one of the four instruments after performing a) the first and b) the second local offset correction. In the plots, the laser spot is scaled to 50% of its nominal size of $15 \mu\text{m}$. After the first offset correction, the measured average targeting accuracy is $\bar{d}_1 = (4.3 \pm 0.8) \mu\text{m}$. This value improves to $\bar{d}_2 = (1.8 \pm 0.7) \mu\text{m}$ if two local offset corrections are done. A third local offset correction did not improve the result further. It is worth noting that \bar{d}_1 and \bar{d}_2 are both much smaller than the laser spot diameter.

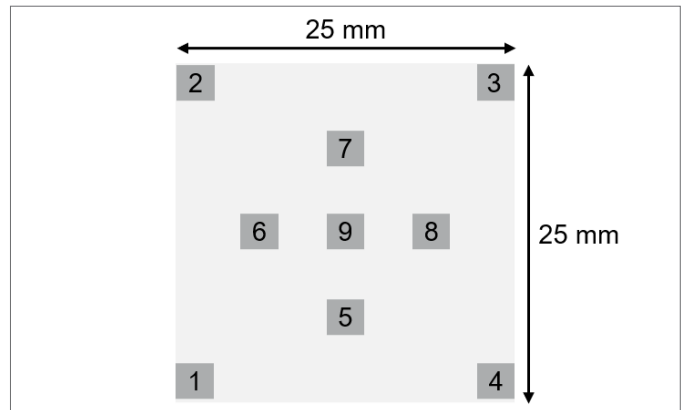


Figure 6: Schematic showing the nine sites for which the laser targeting accuracy was measured after a single and a double offset correction. The sites span an area of $25 \times 25 \text{ mm}$.

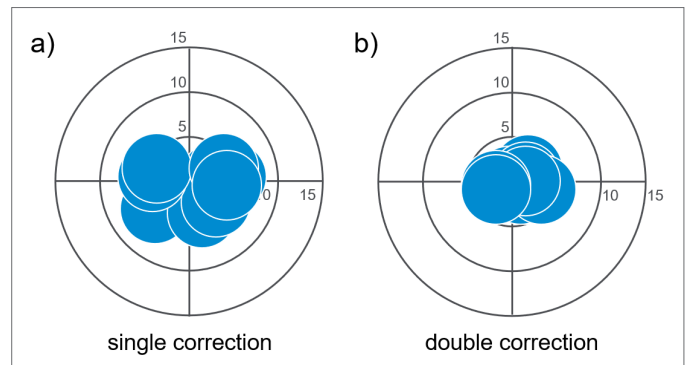


Figure 7: Visualization of the laser targeting accuracy for targets distributed across an area of $25 \times 25 \text{ mm}$ as shown in Figure 6. For clarity, the laser spots are half of their nominal size of $15 \mu\text{m}$.

Site-Specific Sample Preparation Using the Double Local Offset Correction Method – An Example

Figure 8 shows the preparation of a sample for the LEAP (local electrode atom probe) in silicon using the double local offset correction method.

The ROI was marked and protected with a circular IBID of carbon with a $2 \mu\text{m}$ diameter (FIB parameters: 30 kV, 50 pA). Protection of the ROI and FIB machining of the target fiducials (30 kV, 1.5 nA) were done using a pre-stored recipe with a total exposure time of 4 min 17 s. A double local offset correction was done, which took approximately 15 min. A pillar was then laser machined in the sample containing the ROI; see inset of 8b. The laser-machined area has an outer diameter of $500 \mu\text{m}$ and an inner diameter of $38 \mu\text{m}$. The material around the ROI was removed to a depth of $120 \mu\text{m}$ in just 29 s. Subsequently, shaping of the atom probe specimen was done by standard FIB milling using a pattern of concentric rings of decreasing sizes and FIB currents (in the range of 30 nA to 700 pA) centered around the ROI [8] (Fig. 8c). This step added 22 min 29 s to preparation. The final LEAP sample is shown in Figure 8d. It is $20 \mu\text{m}$ tall with a tip radius of 60 nm . The IBID is clearly visible at the top of the tip. The full preparation did not take longer than 45 min.

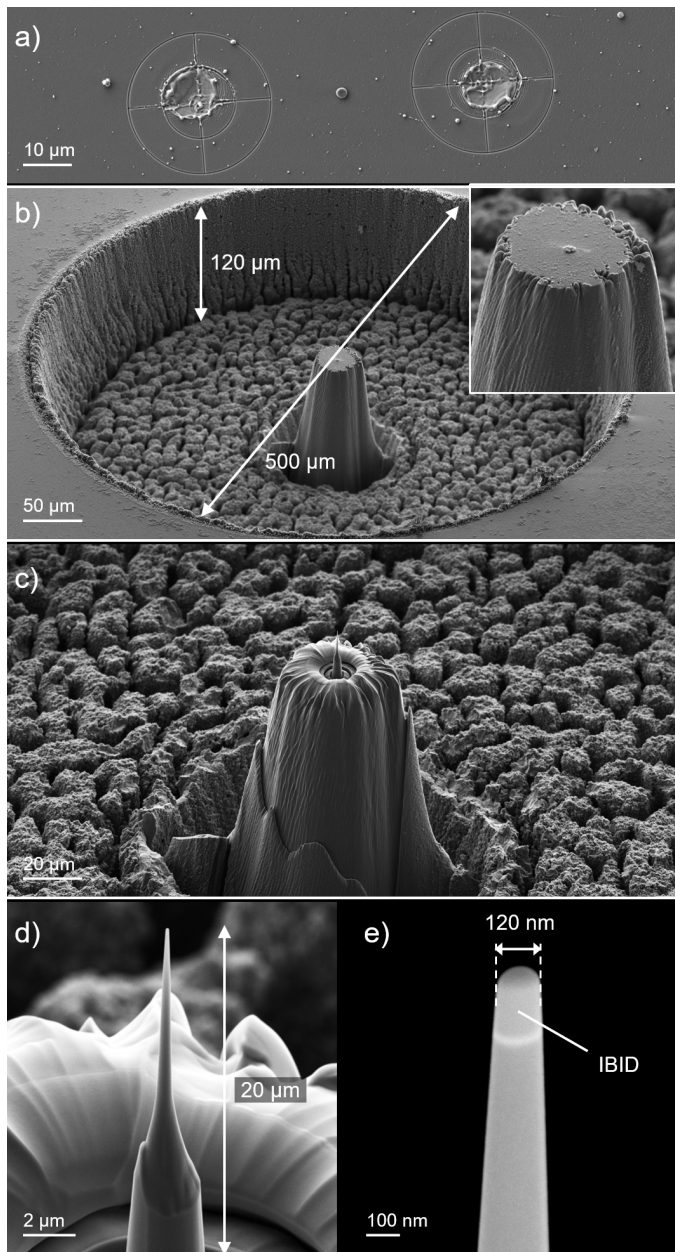


Figure 8: Laser-assisted preparation of a sample for the LEAP. a) The double local offset correction method allows targeting the ROI with better than $2\ \mu\text{m}$ accuracy. b) Sample after the laser machining step. The inset shows the ROI inside the pillar. c) Pillar after the FIB machining step. d) The LEAP sample is $20\ \mu\text{m}$ tall. e) The Inlens SE image shows the IBID. The radius of curvature of the tip is $60\ \text{nm}$.

Summary

In this technical note, we described the laser registration procedure that enables site-specific sample preparation on ZEISS Crossbeam laser.

Different factors limit the achievable laser targeting accuracy. Luckily, the contribution of all these factors but one can be determined experimentally and corrected for using the local offset correction method. After a first local offset correction, the targeting accuracy is improved roughly by a factor of three. With a second iteration, i.e. after a double local offset correction, the laser targeting accuracy can be further improved to better than $2\ \mu\text{m}$.

Such high accuracy allows performing site-specific sample preparation workflows requiring massive material removal and most precise FIB machining very efficiently as illustrated using a sample preparation for the LEAP as an example.

References

- [1] J. Meijer et al., Laser Machining by short and ultrashort pulses, state of the art and new opportunities in the age of the photons, CIRP Ann.Manuf. Technol. 51 (2002), pp. 531–550.
- [2] <https://3d-micromac.com/laser-micromachining/products/microprep/>
- [3] M.P. Echlin et al., The TriBeam system: Femtosecond laser ablation in situ SEM, Mater. Charact. 100 (2015), pp 1–12.
- [4] B. Tordoff et al., The LaserFIB: New Application Opportunities Combining a High-Performance FIB-SEM with Femtosecond Laser Processing in a Second Integrated Chamber, Appl. Microsc. 50 (2020), pp. 1–11.
- [5] The total laser scan range is $40\ \text{x}\ 40\ \text{mm}$.
- [6] <https://www.zeiss.com/microscopy/int/products/microscope-software/zen-intellectis-image-segmentation-by-deep-learning.html>
- [7] www.appeer.com
- [8] FIB-SEM Fabrication of Atom Probe Specimens with ZEISS Crossbeam, ZEISS Application Note (2021), https://zeiss.widen.net/s/bjrw8pjmjs/en_wp_crossbeam_fib-sem_atom_probe_specimens

